Dyes and Pigments 113 (2015) 596–601

Contents lists available at ScienceDirect

Dyes and Pigments

journal homepage: www.elsevier.com/locate/dyepig

Highly selective red-emitting H_2S fluorescent probe with a large Stokes shift

Wenqiang Chen [a], Song Chen [a], Bingjiang Zhou [b], Hongbo Wang [a], Xiangzhi Song [a, c, *], Hongyan Zhang [b, **]

[a] College of Chemistry & Chemical Engineering, Central South University, 932 Lushan South Road, Changsha, Hunan Province, 410083, PR China
[b] Laboratory of Photochemical Conversion and Optoelectronic Materials, Technical Institute of Physics and Chemistry, Chinese Academy of Sciences, Beijing, 100190, PR China
[c] State Key Laboratory of Fine Chemicals, Dalian University of Technology, Dalian, Liaoning Province, 116024, PR China

ARTICLE INFO

Article history:
Received 15 June 2014
Received in revised form
23 September 2014
Accepted 24 September 2014
Available online 2 October 2014

Keywords:
Red-emitting
Large Stokes shift
ESIPT
Fluorescent probe
Hydrogen sulfide
Cell imaging

ABSTRACT

The O-2,4-dinitrobenzensulfonate of 1,3-bis(bispyridin-2ylimino)isoindolin-4-ol has been developed as a novel red-emitting fluorescent probe for the detection of H_2S. The dinitrobenzenesulfonate moiety in the probe both prohibits the excited state intramolecular proton transfer process and produces a photo-induced electron transfer process, which renders the probe non-fluorescent in the absence of the analyte. In the presence of H_2S a specific H_2S-mediated cleavage reaction converts the probe into 1,3-bis(bispyridin-2-ylimino)isoindolin-4-ol which exhibits a strong red fluorescence with a large Stokes shift (218 nm) via an excited state intramolecular proton transfer process upon excitation. It's noteworthy that this new probe shows good selectivity and sensitivity to H_2S over glutathione, cysteine and homocysteine. Moreover successful detection and imaging of intracellular H_2S in living cells was achieved. To our knowledge this is the first application of this type of fluorescent probe for intracellular H_2S detection.

1. Introduction

For several centuries, hydrogen sulfide (H_2S) was conventionally considered as a toxic gas and environmental hazard affecting the nervous, respiratory, and cardiovascular system of mammals [1]. Resembling CO and NO, H_2S has more recently emerged as the third endogenous gasotransmitter and cellular signaling molecule involved in many physiological activities, i.e., regulating the cardiovascular, neuronal, immune, endocrine and gastrointestinal systems [2–5]. Furthermore, H_2S serves as a scavenger for endogenous reactive oxygen species (ROS) [6]. Due to its important roles in human health, abnormal levels of H_2S can lead to serious diseases such as Alzheimer's disease [7] and Down's syndrome [8]. Therefore, interest in the role and detection of H_2S has increased during the last decade. As a consequence, qualitative and quantitative detection of H_2S in living systems is tremendously meaningful.

Owing to its operational simplicity, potential high sensitivity and selectivity, fluorescent sensing as a powerful technique has been frequently used to detect and image H_2S *in vivo* [9]. Many fluorescent H_2S probes have been developed in the past several years [10–14]. Generally, 2,4-dinitrobenzensulfonyl unit is used as a recognition group to construct fluorescent probes for the detection of biothiols (Cys, GSH, Hcy) [15–17]. Since H_2S is more reactive than biothiols, it can also cleave the 2,4-dinitrobenzensulfonyl moiety and previous DNBS-based fluorescent probes didn't show selectivity between H_2S and biothiols [18]. Therefore, to date and to our knowledge, there is no DNBS-based fluorescent probe reported to detect and image intracellular H_2S in living cells due to the interference of biothiols.

It is well known that fluorescent dyes with emission in the red and NIR regions and large Stokes shift are favorable for fluorescence imaging in cells because: 1) photons with longer wavelength tend to reduce environmentally-induced light scattering, be less susceptible to the experiment noise from endogenous chromophores, and usually cause less light-induced organelle damage [19]; 2) the large Stokes shift can highly improve the sensitivity of fluorescence

* Corresponding author. State Key Laboratory of Fine Chemicals, Dalian University of Technology, Dalian, Liaoning Province, 116024, PR China. Tel./fax: +86 731 88836954.
** Corresponding author.
E-mail addresses: xzsong@csu.edu.cn (X. Song), zhanghongyan@mail.ipc.ac.cn (H. Zhang).

http://dx.doi.org/10.1016/j.dyepig.2014.09.035
0143-7208/

microscopy wherein emission photons can be detected against the background from excitation photons [21]. Recently, Thompson et al. reported a class of ESIPT (excited state intramolecular proton transfer) fluorescent dyes involving the 1,3-bis(imino)isoindolediol motif (**BPI**), having an emission in red region (about 600 nm), high quantum yields (up to 45%) and large Stokes shift (>165 nm) [20]. Inspired by these traits of the **BPI** dyes, our group synthesized a new **BPI** dye, 1,3-bis(bispyridin-2ylimino)isoindolin-4-ol (**3**) (shown in Scheme 1), and deliberately studied its photophysical properties. In aqueous solution, reference dye **3** emits bright red lights ($\lambda_{max} = 585$ nm) with a 218 nm Stokes shift (shown in Fig. 1) and is photostable. Considering these advantages, we envision that reference dye **3** might be an excellent candidate upon which fluorescent probes are based.

In this work, we reported a DNBS-based red-emitting fluorescent probe, **BPI-DNBS** (shown in Scheme 1), for the selective and sensitive detection of H_2S. This probe is non-fluorescent in the absence of H_2S. However, the probe rapidly displays a remarkable fluorescence enhancement ($\lambda_{max} = 585$ nm) upon the addition of H_2S. Particularly, biothiols including Cys, Hcy and GSH only induce weak fluorescence signal. To the best of our knowledge, this is the first DNBS-based fluorescent probe to distinguish H_2S from biothiols. The capability of **BPI-DNBS** to visualize intracellular H_2S in living A594 cells has been demonstrated.

2. Experimental

2.1. Chemicals and apparatus

Unless otherwise stated, all reagents were purchased from commercial suppliers and used without further purification. All solvents were purified by standard methods. Twice-distilled water was used throughout all experiments. NMR spectra were recorded on a BRUKER 400 spectrometer, using TMS as an internal standard. FT-IR spectra were recorded on a Thermo Scientific ET6700 FT-IR spectrophotometer. All accurate mass spectrometric experiments were performed on a micrOTOF-Q II mass spectrometer (Bruker Daltonik, Germany). UV–Vis absorption spectra were measured using a Shimadzu UV-2450 spectrophotometer. Emission spectra were recorded at room temperature using a HITACHI F4600 fluorescence spectrophotometer with both the excitation and emission slit widths set at 5.0 nm. Cell imaging was performed with a Nikon

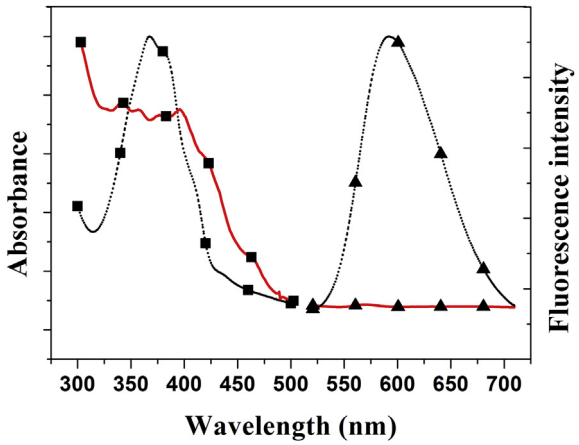

Fig. 1. The absorption (■) and emission spectra (▲) of reference dye **3** and **BPI-DNBS** in HEPES-DMSO solution (20 mM, $v/v = 4:1$, pH = 7.0). Black dotted lines: dye **3**; red solid lines: **BPI-DNBS**. (For interpretation of the references to color in this figure legend, the reader is referred to the web version of this article.)

C1si inverted microscope. TLC analysis was performed on silica gel plates and column chromatography was conducted over silica gel (mesh 200–300), both of which were obtained from Qingdao Ocean Chemicals. The solutions of various testing species were prepared from $NaClO_4 \cdot H_2O$, Na_2SO_4, NaF, KI, NaCl, NaBr, NaN_3, $NaNO_3$, $Na_2S_2O_3 \cdot 5H_2O$, Na_2SO_3, $NaNO_2$, CH_3COONa, Na_2CO_3, $NaBF_4$, KSCN, Hcy, GSH, Cys, H_2O_2, NaClO in twice-distilled water. Density functional theory (DFT) calculations with the B3LYP exchange functional employing 6-31G basis sets using a suite of Gaussian 09 programs were performed.

2.2. Synthesis

The synthetic route of **BPI-DNBS** was shown in Scheme 1. 3-Hydroxypathalonitrile was condensed with 2-aminopyridine to give reference dye **3**, which subsequently reacted with 2,4-dinitrobenzenesulfonyl chloride to afford the fluorescent probe.

2.2.1. Synthesis of compound *2*

3-Hydroxypthalonitrile was synthesized according to the literature method [22]. To a 50 mL round-bottom flask were added 3-

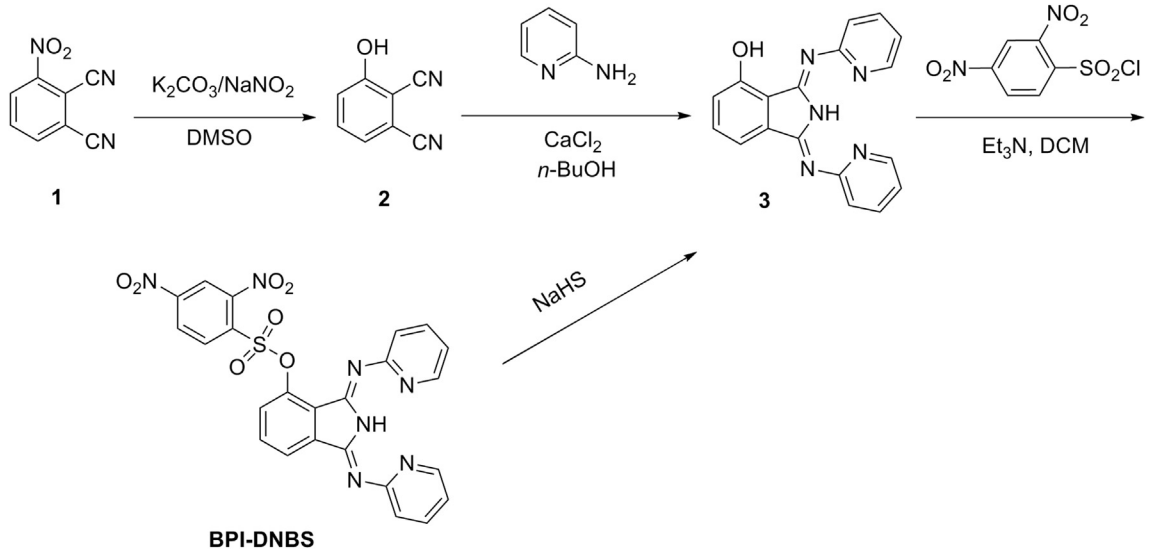

Scheme 1. Synthesis of **BPI-DNBS** and the approach to detecting H_2S.

nitropthalonitrile (2.0 g, 11.6 mmol), K_2CO_3 (1.8 g, 12.7 mmol) and $NaNO_2$ (0.8 g, 11.6 mmol) in DMSO (30 mL), and the reaction mixture was stirred under reflux for 30 min. After cooling to room temperature, the reaction mixture was diluted with water (90 mL) and subsequently acidified with 2 M HCl to pH = 3 to produce a precipitate. Then, the solid was collected by filtration and washed successively with water and methanol. The pure product was obtained by recrystallization in acetic acid as a brown crystal (0.8 g, 48%). Mp: 263–265 °C.

2.2.2. Synthesis of reference dye ***3***

To a 25 mL round-bottom flask were added compound **2** (288 mg, 2 mmol), 2-aminopyridine (385 mg, 4.1 mmol) and $CaCl_2$ (46 mg, 0.41 mmol) in *n*-BuOH (6 mL). The reaction mixture was refluxed under an argon atmosphere for 5 days with stirring. After cooling to room temperature, the precipitate was collected by filtration and washed with water (3 × 20 mL). The obtained solid was further purified by silica gel column chromatography (dichloromethane as eluent) to yield the pure reference dye **3** as an orange yellow powder (68 mg, 12%). Mp: 200–202 °C. ^{1}H NMR (400 MHz, $CDCl_3$) δ 13.70 (s, 1H), 8.62 (m, 2H), 7.78 (t, J = 7.9 Hz, 2H), 7.60 (s, 1H), 7.52 (d, J = 7.3 Hz, 2H), 7.38 (d, J = 8.0 Hz, 1H), 7.19–7.09 (m, 3H). ^{13}C NMR (101 MHz, $CDCl_3$) δ 160.10, 159.34, 155.81, 155.59, 153.70, 147.98, 147.76, 138.12, 138.08, 135.66, 133.58, 123.43, 122.31, 120.50, 120.27, 118.98, 118.29, 114.52. IR (KBr) ν_{max} cm^{-1}: 3446, 1631, 1580, 1550, 1459, 1431, 1309, 1226, 1151, 1057, 790. HRMS (EI) Calcd. for $C_{18}H_{14}N_5O$ ($[M + H]^+$) : 316.1198; Found: 316.1197.

2.2.3. Synthesis of BPI-DNBS

A solution of reference dye **3** (32 mg, 0.1 mmol), 2,4-dinitrobenzenesulfonyl chloride (53 mg, 0.2 mmol) and triethylamine (26 mg, 0.24 mmol) in dichloromethane (5 mL) was stirred at room temperature for 2 h. After the removal of solvent under reduced pressure, the resulting residue was further purified by column chromatography (silica gel, dichloromethane as eluent) to give the target compound, **BPI-DNBS**, as a light yellow solid (16 mg, 30%). Mp: 184–187 °C. ^{1}H NMR (400 MHz, $CDCl_3$) δ 13.83 (s, 1H), 8.57–8.52 (m, 2H), 8.49 (d, J = 9.9 Hz, 2H), 8.37 (d, J = 8.6 Hz, 1H), 8.17 (s, 1H), 7.80 (t, J = 7.7 Hz, 1H), 7.73 (t, J = 7.9 Hz, 2H), 7.55 (d, J = 8.1 Hz, 1H), 7.50 (s, 1H), 7.18–7.10 (m, 2H), 7.04 (d, J = 7.9 Hz, 1H). ^{13}C NMR (101 MHz, $CDCl_3$) δ 159.6, 150.3, 148.8, 148.0, 147.7, 144.2, 138.3, 138.1, 135.1, 133.7, 133.2, 127.1, 126.8, 126.1, 123.4, 122.6, 120.8, 120.7, 120.0. IR (KBr) ν_{max} cm^{-1}: 3453, 3034, 1630, 1579, 1558, 1458, 1391, 1357, 1262, 1200, 1171, 1097, 1047, 962, 800, 732. HRMS (EI) Calcd. for $C_{24}H_{16}N_7O_7S$ ($[M + H]^+$): 546.0832; Found: 546.0817.

2.3. Absorption and fluorescence spectroscopy

The stock solution of the probe, **BPI-DNBS**, was prepared at 1 mM in DMSO. The test solution of **BPI-DNBS** (5.0 μM) in 2 mL of 20 mM HEPES buffer (20 mM, pH = 7.0) was prepared by placing 0.01 mL stock solution of **BPI-DNBS** and 0.39 mL DMSO in 1.59 mL HEPES buffer. The resulting solution was shaken well and incubated with 0.01 mL appropriate testing species for 60 min at 37 °C before recording the spectra. For all measurements of fluorescence spectra, excitation wavelength was set at 368 nm and the scan speed is 1200 nm min^{-1}.

2.4. Cell culture and fluorescence confocal imaging

A549 was gifted from the center of cells, Peking Union Medical College. Cells were grown in McCoy'5A, supplemented with 10% fetal bovine serum and 1% penicillin/streptomycin, incubated under 5% CO_2 at 37 °C. Cells were seeded on confocal dish for imaging 24 h prior to conducting the experiments. Before the experiments, the cells were washed with HEPES buffer solution. A549 cells were then incubated with a solution of **BPI-DNBS** (5.0 μM in HEPES buffer containing 1% DMSO) at 37 °C for 30 min. After washing 3 times with HEPES buffer, the pretreated A549 cells were then incubated with NaHS (200.0 μM) for another 30 min. Fluorescence imaging was performed with excitation wavelength at 405 nm using Cy3 channel. For a control experiment, A549 cells were incubated with the solution of **BPI-DNBS** (5.0 μM) in the culture medium at 37 °C for 30 min, and the fluorescence imaging was carried out after washing the cells with HEPES buffer 3 times.

3. Results and discussion

3.1. Spectroscopic evaluation of reference dye 3 and BPI-DNBS

The photophysical properties of reference dye **3** and **BPI-DNBS** were investigated in HEPES-DMSO solution (20 mM, v/v = 4:1, pH = 7.0). As shown in Fig. 1, reference dye **3** absorbs at 367 nm and emits at 585 nm. The extremely large Stokes shift (218 nm) was ascribed to the effective ESIPT process from the hydroxyl proton to the imine nitrogen. The fluorescent quantum yield of reference dye **3** was 3.8% in HEPES-DMSO solution (coumarin 1 in EtOH with Φ_f = 0.73 as a reference) [23]. However, **BPI-DNBS** displays an absorption band centered at 396 nm with a faint yellow color. In **BPI-DNBS**, the ESIPT process was inhibited by the **DNBS** protection, which can strongly quench the fluorescence. Moreover, the density function theory calculations showed that the LUMO energy level (−0.084 eV) of reference dye **3** is higher than that of dinitrobenzene (−0.134 eV) moiety (Fig. 2). Thus, the photo-induced electron transfer (PET) process from the excited reference dye **3** to the dinitrobenzene moiety is thermodynamically favorable, which also leads to the effective fluorescence quenching. Due to the inhibition of ESIPT and the effective PET process, **BPI-DNBS** is essentially non-fluorescent (not detectable).

3.2. Sensing response of BPI-DNBS to H_2S

First, we investigated the UV–vis absorption spectral changes of **BPI-DNBS** in response to H_2S. The addition of H_2S with an increasing amount to the solution of **BPI-DNBS** (5.0 μM) gradually elicited a blue shift to 367 nm in its absorption spectra, which is

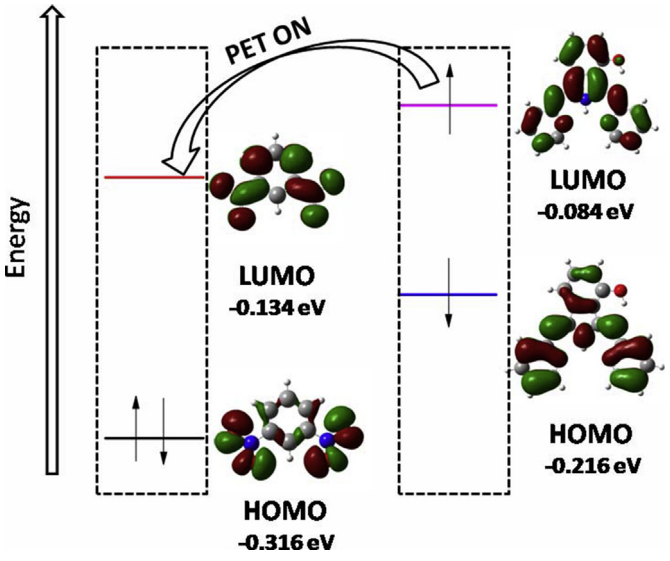

Fig. 2. Frontier orbital diagrams of reference dye **3** (the dye scaffold) and dinitrobenzene (the PET switch) for the probe **BPI-DNBS**. Orbital energies were calculated by using Gaussian 09 program in B3LYP/6-31G level.

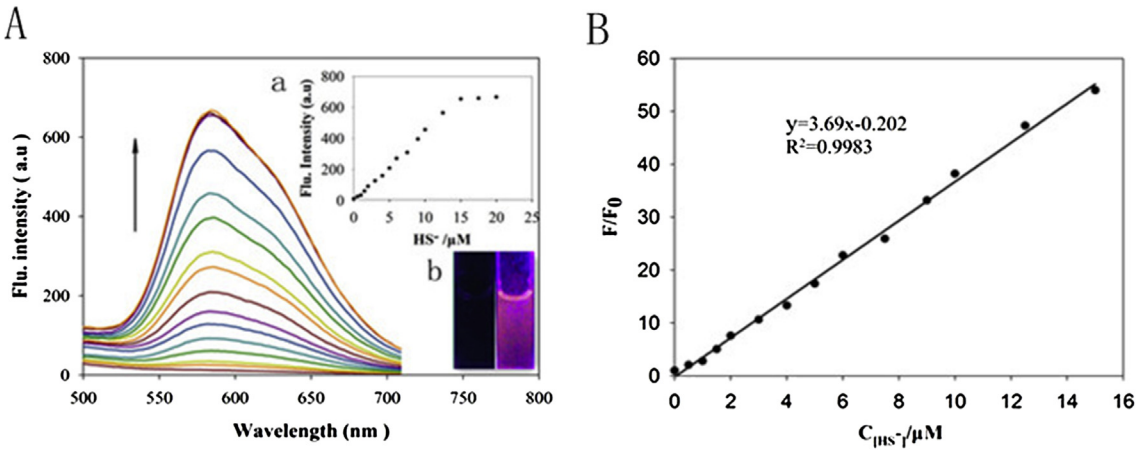

Fig. 3. A) Fluorescence spectra of **BPI-DNBS** (λ_{ex} = 368 nm, 5.0 μM) upon the addition of NaHS (0.0–20.0 μM) in HEPES-DMSO solution (v/v = 4:1, pH = 7.0). Inset: a) fluorescence intensity at 585 nm of **BPI-DNBS** (5.0 μM) as a function of NaHS concentration; b) fluorescence images of **BPI-DNBS** in the absence (left) and presence of NaHS (right). B) Fluorescence intensity ratio (F/F_0) at 585 nm of **BPI-DNBS** (5.0 μM) as a function of NaHS concentration in HEPES-DMSO solution (20 mM HEPES, v/v = 4:1, pH = 7.0).

quite similar to the absorption spectra of reference dye **3** (Fig. S2). The emission spectra of **BPI-DNBS** toward H_2S in HEPES-DMSO solution (20 mM, v/v = 4:1, pH = 7.0) are displayed in Fig. 3. The solution of **BPI-DNBS** rapidly exhibits a strong red fluorescence enhancement (up to 55-fold) upon the treatment of H_2S. The fluorescence spectrum of the reaction product is identical to that of reference dye **3**. The UV–vis and fluorescence studies clearly indicated that H_2S could effectively cleave 2,4-dinitrobenzensulfonate unit in **BPI-DNBS**, generating reference dye **3** which displays a strong red fluorescence upon excitation (shown in Scheme 1). Inspection of Fig. 3 shows that the fluorescence intensity at 585 nm increased with increasing the H_2S concentrations (0–15 μM) with a good linearity, R = 0.9983. Specifically, the addition of 1.0 μM H_2S could result in a fluorescence enhancement more than 3 folds (Fig. S3). The detection limit was calculated to be 1.5×10^{-8} mol L^{-1} under experimental conditions (S/N = 3). Thus, it can be concluded that **BPI-DNBS** is highly sensitive to H_2S.

3.3. Selectivity studies

To evaluate the selectivity of this probe, we then measured the fluorescence response of **BPI-DNBS** to typical anions and other biologically relevant species. As shown in Fig. 4, the fluorescent probe exhibits negligible fluorescence in response to the representative anions (AcO^-, BF_4^-, Br^-, Cl^-, ClO_4^-, CO_3^{2-}, F^-, I^-, N_3^-, NO_2^-, NO_3^-, SO_4^{2-}, SCN^-), reactive oxygen (ClO^-, H_2O_2), and reducing anions ($S_2O_5^{2-}$, $S_2O_3^{2-}$, SO_3^{2-}). It's noteworthy that biothiols (Cys, Hcy and GSH) only produce a weak fluorescence signal even at a high concentration (200.0 μM for Cys, Hcy and GSH). The results demonstrate that **BPI-DNBS** can be used to detect H_2S with good selectivity over biothiols, which makes it capable of detecting H_2S in living cells. This selectivity might be attributed to the differences of molecular size and *p*Ka between H_2S and biothiols. First, due to the steric effect by the adjacent pyridinyl group in **BPI-DNBS**, H_2S can effect the thiolysis of 2,4-dinitrobenzensulfonate more effectively than biothiols owing to its smaller size. Second, the *p*Ka of H_2S is 6.9 in aqueous solution whereas it is approximately around 8.5 for biothiols. Thus, at physiological pH value, H_2S mainly exists in the more reactive form, HS^-, and can readily react with the probe [24,25]. Ongoing studies are being performed in our laboratory to prove this postulation.

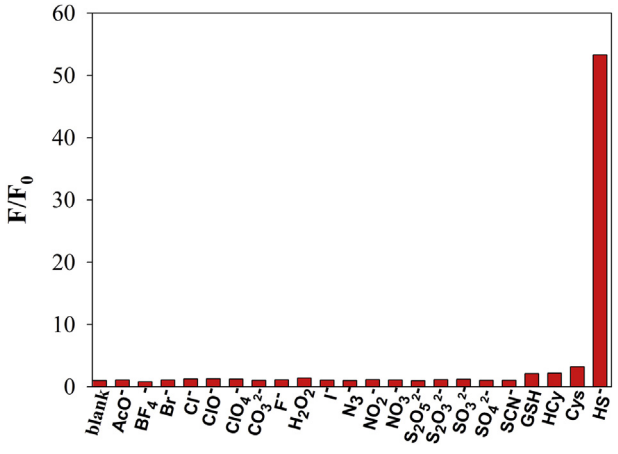

Fig. 4. Fluorescence intensity ratio (F/F_0) at 585 nm of the probe **BPI-DNBS** (5.0 μM) in response to various anions, reactive oxygen species, reducing agents, biothiols and NaHS (20.0 μM for AcO^-, BF_4^-, Br^-, Cl^-, ClO_4^-, CO_3^{2-}, F^-, I^-, N_3^-, NO_2^-, NO_3^-, SO_4^{2-}, SCN^-, $S_2O_5^{2-}$, $S_2O_3^{2-}$ and SO_3^{2-}; 50.0 μM for ClO^- and H_2O_2; 200.0 μM for GSH, Hcy and Cys; 20.0 μM for NaHS).

3.4. Effect of pH on fluorescence detection of H_2S

In order to confirm the practical applicability of **BPI-DNBS**, we further investigate the influence of pH on the fluorescence of this probe. It can be seen in Fig. 5 that **BPI-DNBS** shows little

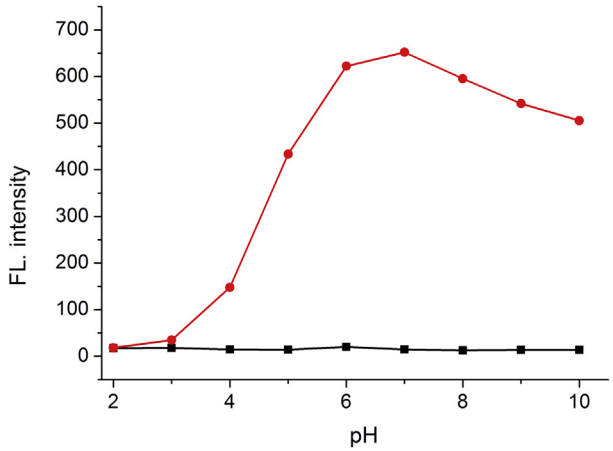

Fig. 5. pH effect on the fluorescence intensity at 585 nm of **BPI-DNBS** (5.0 μM) in the absence (black line) and presence (red line) of NaHS (20.0 μM) in H_2O-DMSO solution (v/v = 4:1). (For interpretation of the references to color in this figure legend, the reader is referred to the web version of this article.)

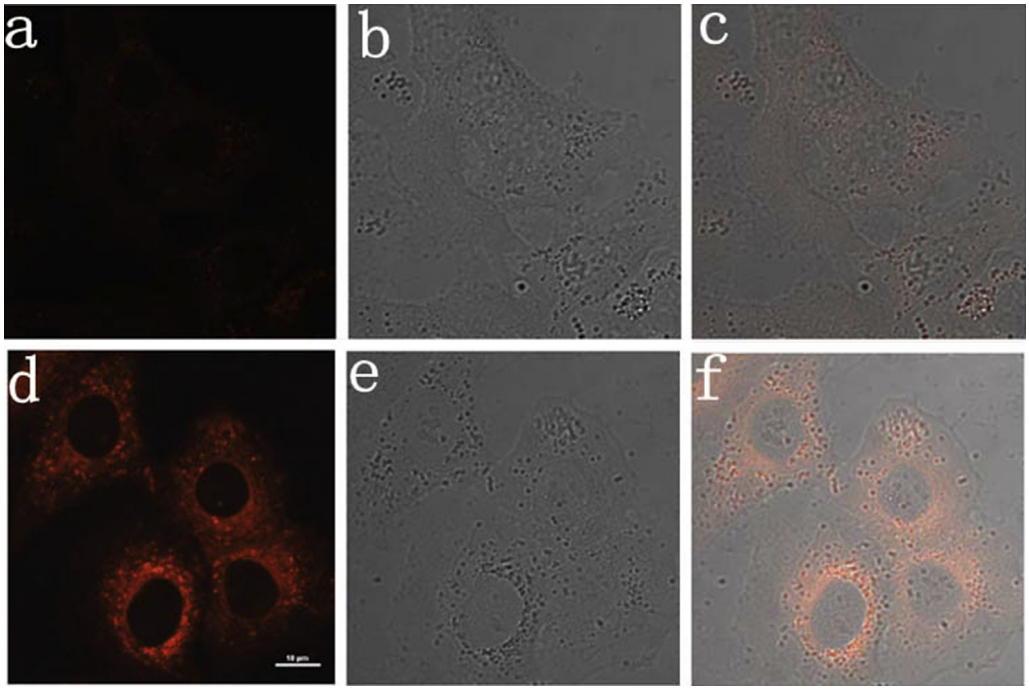

Fig. 6. Confocal fluorescence contrast images of living A594 cells incubated with 5.0 μM **BPI-DNBS** for 30 min at 37 °C (top row) and further treated with 200.0 μM NaHS for 30 min at 37 °C (bottom row). (a, d) Fluorescence images; (b, e) bright field images; (c, f) fluorescence and bright field overlay images. Scale bar = 10 μm.

fluorescence within a wide pH range (1–10), indicating that this fluorescent probe is stable between pH 1–10. When treated with 5 equivalents of H_2S, **BPI-DNBS** displays a strong fluorescence between pH 6–8. This result suggested that **BPI-DNBS** could work effectively under physiological condition.

3.5. Cell imaging

Finally, we applied **BPI-DNBS** to capture H_2S in living A594 cells (human lung cancer cells), as shown in Fig. 6. When A594 cells were incubated with 5.0 μM **BPI-DNBS** for 30 min at 37 °C and then washed twice with PBS buffer, only weak fluorescence was observed due to the weak response to biothiols. However, intense red fluorescence in cells emerged when similar treated cells were further incubated with NaHS (200.0 μM) for 30 min at 37 °C. This result indicated that **BPI-DNBS** was permeable to cell membrane and able to response to endogenous H_2S in living cells.

4. Conclusions

In summary, we have successfully developed a novel red-emitting H_2S fluorescence probe employing a 2,4-dinitrosulfonyl moiety as the sensing group (λ_{max}em = 585 nm). This probe displays a large Stokes shift (218 nm) in response to H_2S that is beneficial for signal detection in fluorescence microscopy. It's noteworthy that this DNBS-based probe is highly sensitive and selective toward H_2S against biothiols and other relevant ions. Importantly, **BPI-DNBS** displayed good cell permeability and was successfully applied to visualize intracellular H_2S in living cells.

Acknowledgments

The research was supported by the Fundamental Research Funds for the Central Universities, the State Key Laboratory of Fine Chemicals (KF1202) and the Hunan Nonferrous Fund (No. YSZN2013CL02). We thank Modern Analysis and Testing Center of CSU for NMR spectral data of all the compounds.

Appendix A. Supplementary data

Supplementary data related to this article can be found at http://dx.doi.org/10.1016/j.dyepig.2014.09.035.

References

[1] Beauchamp RO, Bus JS, Popp JA, Boreiko CJ, Andjelkovich DA, Leber P. A critical review of the literature on hydrogen sulfide toxicity. CRC Crit Rev Toxicol 1984;13:25–97.
[2] Villa Bianca RE, Sorrentino R, Mirone V, Cirino G. Hydrogen sulfide and erectile function: a novel therapeutic target. Nat Rev Urol 2011;8:286–9.
[3] Miller TW, Isenberg JS, Roberts DD. Molecular regulation of tumor angiogenesis and perfusion via redox signaling. Chem Rev 2009;109:3099–124.
[4] Szabo C. Gaseotransmitters: new frontiers for translational science. Sci Transl Med 2010;2:54–8.
[5] Wang R. The gasotransmitter role of hydrogen sulfide. Antioxid Redox Signal 2003;5:493–501.
[6] Calvert JW, Jha S, Gundewar S, Elrod JW, Ramachandran A, Pattillo CB, et al. Hydrogen sulfide mediates cardioprotection through Nrf2 signaling. Circ Res 2009;105:365–74.
[7] Eto K, Asada T, Arima K, Makifuchi T, Kimura H. Brain hydrogen sulfide is severely decreased in Alzheimer's disease. Biochem Biophys Res Commun 2002;293:1485–8.
[8] Kamoun P, Belardinelli MC, Chabli A, Lallouchi K, Chadefaux-Vekemans B. Endogenous hydrogen sulfide overproduction in down syndrome. Am J Med Genet A 2003;116:310–1.
[9] Kim JS, Quang DT. Calixarene-derived fluorescent probes. Chem Rev 2007;107:3780–99.
[10] Peng H, Cheng Y, Dai C, King AL, Predmore BL, Lefer DJ, et al. A fluorescent probe for fast and quantitative detection of hydrogen sulfide in blood. Angew Chem Int Ed 2011;50:9672–5.
[11] Lippert AR, New EJ, Chang CJ. Reaction-based fluorescent probes for selective imaging of hydrogen sulfide in living cells. J Am Chem Soc 2011;133:10078–80.
[12] Sasakura K, Hanaoka K, Shibuya N, Mikami N, Kimura Y, Komatsu T, et al. Development of a highly selective fluorescence probe for hydrogen sulfide. J Am Chem Soc 2011;133:18003–5.
[13] Liu C, Pan J, Li S, Zhao Y, Wu LY, Berkman CE, et al. Capture and visualization of hydrogen sulfide by a fluorescent probe. Angew Chem Int Ed 2011;123:10511–3.
[14] Chen Y, Zhu C, Yang Z, Chen J, He Y, Jiao Y, et al. A ratiometric fluorescent probe for rapid detection of hydrogen sulfide in mitochondria. Angew Chem Int Ed 2013;125:1732–5.
[15] Maeda H, Matsuno H, Ushida M, Katayama K, Saeki K, Itoh N. 2,4-Dinitrobenzenesulfonyl fluoresceins as fluorescent alternatives to Ellman's reagent in thiol-quantification enzyme assays. Angew Chem Int Ed 2005;44:2922–5.

[16] Bouffard J, Kim Y, Swager TM, Weissleder R, Hilderbrand SA. A highly selective fluorescent probe for thiol bioimaging. Org Lett 2008;10:37–40.
[17] Shao J, Guo H, Ji S, Zhao J. Styryl-BODIPY based red-emitting fluorescent OFF–ON molecular probe for specific detection of cysteine. Biosens Bioelectron 2011;26:3012–7.
[18] Yang XF, Wang L, Xu H, Zhao M. A fluorescein-based fluorogenic and chromogenic chemodosimeter for the sensitive detection of sulfide anion in aqueous solution. Anal Chim Acta 2009;631:61–5.
[19] Yuan L, Lin W, Yang Y, Chen H. A unique class of near-infrared functional fluorescent dyes with carboxylic-acid-modulated fluorescence ON/OFF switching: rational design, synthesis, optical properties, theoretical calculations, and applications for fluorescence imaging in living animals. J Am Chem Soc 2012;134:1200–11.
[20] Hanson K, Patel N, Whited MT, Djurovich PI, Thompson ME. Substituted 1,3-bis(imino)isoindole diols: a new class of proton transfer dyes. Org Lett 2011;13:1598–601.
[21] Hou P, Chen S, Wang H, Wang J, Voitchovskya K, Song X. An aqueous red emitting fluorescent fluoride sensing probe exhibiting a large Stokes shift and its application in cell imaging. Chem Commun 2014;50:320–2.
[22] Ranta J, Kumpulainen T, Lemmetyinen H, Efimov A. Synthesis and characterization of monoisomeric 1,8,15,22-substituted (A3B and A2B2) phthalocyanines and phthalocyanine-fullerene dyads. J Org Chem 2010;75:5178–94.
[23] Jones G, Jackson WR, Choi C. Solvent effects on emission yield and lifetime for coumarin laser dyes. Requirements for a rotatory decay mechanism. J Phys Chem 1985;89:294–300.
[24] Mathai JC, Missner A, Kügler P, Saparov SM, Zeidel ML, Lee JK, et al. No facilitator required for membrane transport of hydrogen sulfide. Proc Natl Acad Sci U S A 2009;106:16633–8.
[25] Salinas CN, Anseth KS. Mixed mode thiol acrylate photopolymerizations for the synthesis of PEG peptide hydrogels. Macromolecules 2008;41:6019–26.